



# In Vivo Gold Complex Catalysis within Live Mice

Kazuki Tsubokura<sup>+</sup>, Kenward K. H. Vong<sup>+</sup>, Ambara R. Pradipta, Akihiro Ogura, Sayaka Urano, Tsuyoshi Tahara, Satoshi Nozaki, Hirotaka Onoe, Yoichi Nakao, Regina Sibgatullina, Almira Kurbangalieva, Yasuyoshi Watanabe, and Katsunori Tanaka\*

**Abstract:** Metal complex catalysis within biological systems is largely limited to cell and bacterial systems. In this work, a glycoalbumin–Au<sup>III</sup> complex was designed and developed that enables organ-specific, localized propargyl ester amidation with nearby proteins within live mice. The targeted reactivity can be imaged through the use of Cy7.5- and TAMRA-linked propargyl ester based fluorescent probes. This targeting system could enable the exploitation of other metal catalysis strategies for biomedical and clinical applications.

The use of metal complex catalysts within living biological systems is an area of research that has recently gained significant attention.<sup>[1]</sup> Viewed as alternative chemical tools complementary to traditional bioorthogonal reactions, metal-mediated reactions have potential utility for biological sensing, imaging, and caging applications. However, the implementation of metal complex catalysis is crucially dependent on achieving the right balance: minimizing reactivity towards water, air, and cellular components that are present at high concentrations while also maximizing reactivity towards low cellular concentrations of desired substrates.

Current examples of metal-catalyzed reactions in biological settings (Table 1) include ruthenium-mediated uncaging of allyl carbamates<sup>[2]</sup> and protein labeling,<sup>[3]</sup> iron-mediated

uncaging of azide groups,<sup>[4]</sup> palladium-mediated uncaging of allenyl,<sup>[5]</sup> propargyloxycarbonyl,<sup>[6]</sup> and allyl carbamate groups,<sup>[7]</sup> as well as palladium-mediated N-dealkylation,<sup>[6c]</sup> Suzuki–Miyaura,<sup>[6c,7b,8]</sup> and Sonogashira<sup>[9]</sup> cross-couplings, and gold-mediated hydroarylation cyclizations.<sup>[10]</sup> In addition, in vivo cell-based examples of copper-catalyzed azide–alkyne cycloaddition<sup>[11]</sup> and palladium-mediated carbon monoxide triggered carbonylation also exist.<sup>[12]</sup>

Although pioneering studies have been reported in this field, it has been largely limited to either cell or bacterial systems, the only exception being two studies where metal resins were directly injected into the embryo yolks of zebrafish.<sup>[6e,11]</sup> In order for metal complex catalysts to become therapeutically applicable, one major obstacle that has to be addressed is how to localize metal complexes to specific diseased organs or tumors before they are metabolized and excreted. None of the aforementioned methods sufficiently addresses noninvasive targeting, and no examples have been reported with fully developed organisms.

Herein, we describe a metal-mediated reaction performed within a fully developed living animal. To achieve organ-specific localized reactivity, a glycoalbumin targeting system was employed; structure and multivalency effects of attached asparagine-linked glycans (N-glycans) help facilitate rapid translocation to target organs. Albumin-linked cyclometalated Au<sup>III</sup> complexes were shown to catalyze amide bond formation between fluorescent propargyl ester probes and nearby surface-protein amines (e.g., lysine side chains), enabling local visualization of targeted organs.

Previously, our laboratory developed an innovative targeting method based on N-glycoalbumins (Figure 1 A), which were readily synthesized by immobilizing ten N-glycan molecules onto albumin through the “RIKEN click” reaction.<sup>[13]</sup> Changing the attached N-glycan structure had a direct impact on the trafficking pathways, leading to organ-selective accumulation (e.g., in the liver, intestine, spleen, and even tumors).<sup>[13a–d]</sup> One advantage of this approach is that translocation of the metal complexes to target organs proceeds rapidly (within less than a few hours), thus limiting unwanted internalization or metabolism. For example, we have observed that within 30 min,  $\alpha(2-6)$ -disialoglycoalbumins are retained within the liver for eventual urinary excretion while galactose-terminated glycoalbumins are rapidly trafficked to the intestines. In contrast, the use of antibodies as a targeting system may take as much as 24 h to develop significant levels of accumulation for biological applications.<sup>[14]</sup>

To introduce therapeutic applicability, this work explores the adaptation and usage of organ-targeting glycoalbumins as biologically compatible metal carriers (Figure 1 B). To pro-

[\*] K. Tsubokura,<sup>[+]</sup> Dr. K. K. H. Vong,<sup>[+]</sup> Dr. A. R. Pradipta, Dr. A. Ogura, S. Urano, Dr. K. Tanaka

Biofunctional Synthetic Chemistry Laboratory, RIKEN  
2-1 Hirosawa, Wako-shi, Saitama, 351-0198 (Japan)  
E-mail: kotzenori@riken.jp

Dr. T. Tahara, Dr. S. Nozaki, Dr. H. Onoe, Dr. Y. Watanabe  
RIKEN Center for Life Science Technologies  
6-7-3 Minatojima-minamimachi, Chuo-ku,  
Kobe, Hyogo, 650-0047 (Japan)

K. Tsubokura,<sup>[+]</sup> Dr. Y. Nakao  
Department of Chemistry and Biochemistry  
School of Advanced Science and Engineering, Waseda University  
3-4-1 Okubo, Shinjuku-ku, Tokyo, 169-8555 (Japan)

R. Sibgatullina, Dr. A. Kurbangalieva, Dr. K. Tanaka  
Biofunctional Chemistry Laboratory  
A. Butlerov Institute of Chemistry  
Kazan Federal University  
18 Kremlyovskaya Street, Kazan, 420008 (Russia)

Dr. K. Tanaka  
JST-PRESTO  
2-1 Hirosawa, Wako-shi, Saitama, 351-0198 (Japan)

[+] These authors contributed equally to this work.

Supporting information for this article can be found under:  
<http://dx.doi.org/10.1002/anie.201610273>.



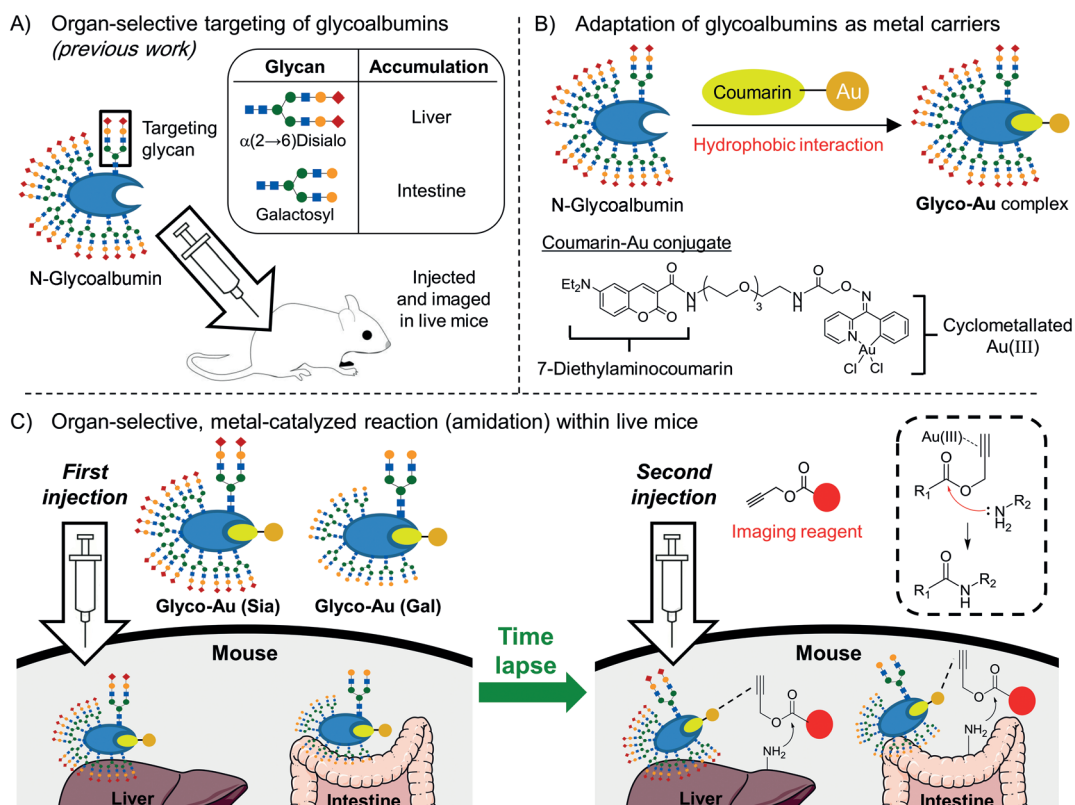


**Figure 1.** A) Organ-selective accumulation within live mice directed by disialo- and galactosyl-linked glycoalbumins. B) Preparation of glycoalbumins as “transition-metal carriers” to produce Glyco-Au complexes. Glyco-Au (Sia) and Glyco-Au (Gal) were synthesized with  $\alpha(2-6)$ -disialoglycoalbumin and galactosylglycoalbumin, respectively (see Figure S1 B for the glycan structures). C) General scheme for liver- and intestine-selective in vivo fluorescence labeling by Au<sup>III</sup>-catalyzed amide bond formation between propargyl ester based imaging probes and surface amino groups of targeted tissues.

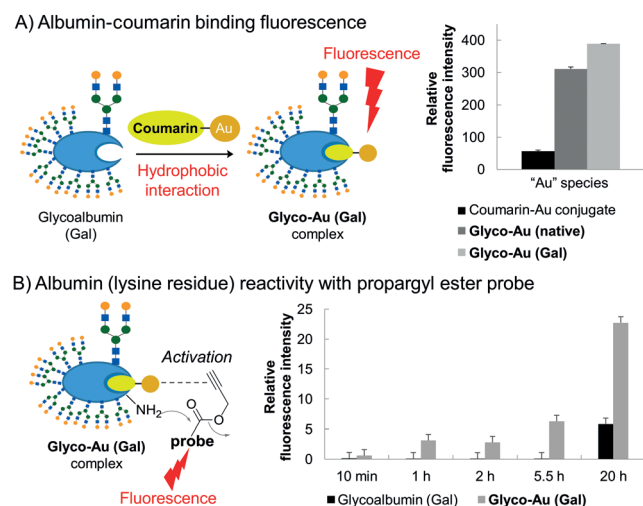


**Figure 2.** A) Changes in the relative fluorescence intensity of the coumarin–Au conjugate upon incorporation into the Glyco-Au (native) and Glyco-Au (Gal) complexes. Equimolar amounts (1 mM) were incubated in H<sub>2</sub>O/DMSO (4:1) at 37°C for 1 h before fluorescence measurement ( $\lambda_{\text{ex}} = 438$  nm,  $\lambda_{\text{em}} = 479$  nm). B) Time-dependent reactivity between TAMRA-OProp and free amines on the protein surfaces in the presence of Glyco-Au (Gal) or the coumarin–Au conjugate lacking glycoalbumin (Gal). The two reactants were incubated in a ratio of 1:10 in H<sub>2</sub>O/DMSO (4:1) at 37°C for the specified time intervals before fluorescence measurement ( $\lambda_{\text{ex}} = 560$  nm,  $\lambda_{\text{em}} = 585$  nm).

between free amines on the glycoalbumin protein surface (e.g., lysine side chains) and a fluorescent propargyl ester probe, such as TAMRA-OProp (Figure 2B and Figure S2A) or Cy7.5-OProp (Figure S2B). TAMRA-OProp was incubated with either the glycoalbumin–metal complex (Glyco-Au (Gal)) or just the glycoalbumin protein alone (Glycoalbumin (Gal)) in a ratio of 1:10 (for the equimolar reaction, see Figure S2A) as shown in Figure 2B. A time-dependent increase in fluorescence was observed following Glyco-Au (Gal) addition to TAMRA-OProp, which strongly suggests that gold-mediated amidation between TAMRA-OProp and free amines on the Glyco-Au (Gal) protein surface has occurred. The background fluorescence observed after extended periods of time (e.g., 20 h) was attributed to nonspecific binding of the TAMRA dye to hydrophobic binding pockets of albumin (Figure S2C). In addition, MALDI-TOF mass-spectrometric analysis of the TAMRA-linked Glyco-Au product gave a protein mass that corresponds to the conjugation of about six TAMRA molecules after 20 h (Figure S3).

To evaluate Glyco-Au catalyzed fluorescent labeling at targeted organs, whole-body fluorescence imaging was employed followed by microscopic analysis of dissected tissues. A protocol with optimized reagent concentrations (other concentrations shown in Figure S4) was developed where the  $\alpha(2-6)$ -disialo- and galactose-terminated glycoal-

bumins complexed with the coumarin–Au conjugate, Glyco-Au (Sia) and Glyco-Au (Gal), were first injected into BALB/cAJcl-nu/nu mice via the tail vein. After 30 min for glycan-directed organ accumulation, the propargyl ester imaging probe Cy7.5-OProp was then introduced. This imaging probe serves as a near-infrared fluorophore for whole-body imaging. Noninvasive fluorescence imaging was then performed over 2 hours using an IVIS® imaging system under anesthesia (Figure 3A–C and Figures S5 and S6). As a control, mice were also treated with the gold-deficient glycoalbumin (Sia) complex and Cy7.5-OProp, where the probe was immediately distributed over the whole body through the capillary vessels on the skin before gradual excretion (Figure 3A). These *in vivo* kinetics are typical for small molecules. In contrast, when Glyco-Au (Sia) or Glyco-Au (Gal) were administered, fluorescence signals from the abdominal region clearly revealed targeted organ labeling dependent on the type of N-glycan linked onto the albumin protein;  $\alpha(2-6)$ -disialoglycans led to liver localization while galactose-terminated glycans gave intestine localization (Figure 3B,C). Our claims were further substantiated by the fluorescence ratios of liver and intestine based on the region of interest (ROI) within a whole body 2 hours after Cy7.5-OProp administration. These data clearly show higher fluorescence intensities for the liver or intestine when Glyco-Au (Sia) or Glyco-Au (Gal), respectively, were used (Figure 3D).

Based on previous *in vivo* imaging experiments with N-glycoalbumins, both  $\alpha(2-6)$ -disialo- and galactose-terminated glycoalbumins are known to be initially captured by the asialoglycoprotein receptor on liver parenchymal cells.<sup>[18]</sup> However, their trafficking pathways differ in that Glyco-Au (Sia) is subject to prolonged retention within the liver (before eventual metabolism and urinary excretion), while stronger interactions between Glyco-Au (Gal) and the asialoglycoprotein receptor cause immediate internalization through endocytosis, leading to transportation through the gall bladder to the intestines. With this knowledge on the trafficking pathways, we propose that the observed fluorescence signals for the glycoalbumin-targeted organs are due to Au<sup>III</sup>-catalyzed amide bond formation with the imaging probes. As further evidence, sliced liver tissues obtained from mice administered with Glyco-Au (Sia) and TAMRA-OProp were analyzed by fluorescence microscopy (Figure 3E–G). For microscopy analysis, TAMRA provides clearer signaling and contrast. The fluorescence intensities (Figure 3G) were clearly higher for tissues obtained from mice injected with Glyco-Au (Sia)/TAMRA-OProp than for the control group (TAMRA-OProp injection only). Furthermore, the fluorescence was observed to be concentrated at the central vein (Figure 3F) where the asialoglycoprotein receptor (target of  $\alpha(2-6)$ -disialoglycoalbumins) is known to be expressed. Additional validation for organ-localized reactivity was obtained by an experiment where liver tissues were homogenized and run on an SDS-PAGE gel (Figure S7). In this experiment, fluorescence smearing indicates that numerous proteins have undergone conjugation. With regard to the intestinal tissues, although slices could not be prepared owing to technical limitations, noninvasive fluorescence imaging and the liver slice data should be enough to directly support our

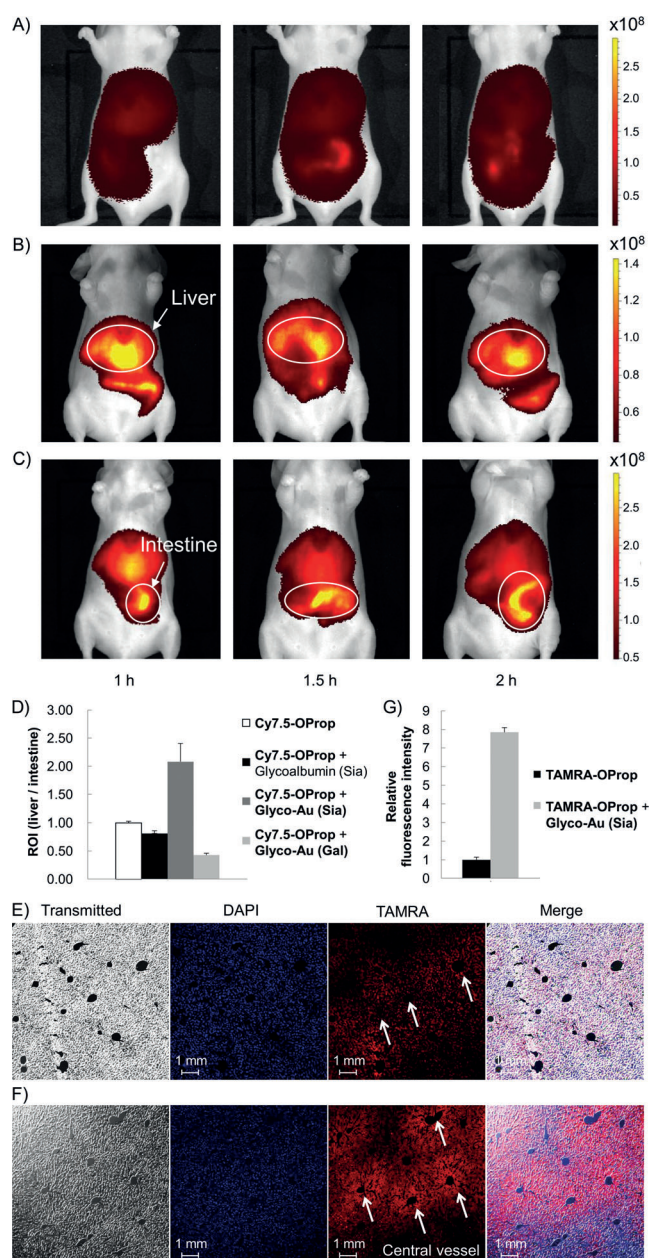


**Figure 3.** Time-course imaging of liver- and intestine-selective fluorescence labeling of BALB/c nude mice (abdominal view) treated with A) glycoalbumin (Sia) followed by Cy7.5-OProp, B) Glyco-Au (Sia) followed by Cy7.5-OProp, and C) Glyco-Au (Gal) followed by Cy7.5-OProp. The Glyco-Au complexes (3.4 nmol) or glycoalbumin as a control were injected into eight to ten week old BALB/cAJcl-nu/nu mice via the tail vein ( $N=6$ ). After 30 min, Cy7.5-OProp or TAMRA-OProp (5.0 nmol) was subsequently injected. The mice were then anesthetized with pentobarbital or isoflurane and placed in a fluorescence imager, where images were taken at 30 min intervals. After 2 h of observation, the mice were sacrificed and perfused with 4% paraformaldehyde solution, and the fluorescence intensity in the liver was measured. D) Fluorescence ratios for the liver and intestine within a whole body 2 h after administration of Cy7.5-OProp. The fluorescence was calculated within an arbitrarily defined region of interest (ROI). Fluorescence microscopy analysis of dissected liver tissue of mice treated with E) only TAMRA-OProp or F) Glyco-Au (Sia) followed by TAMRA-OProp. G) Comparison of the fluorescence intensities between tissue samples of (E) and (F). Mean values with standard errors normalized to the control are given.

claims of the first example of organ-selective, metal-catalyzed reactions in living animals.

In summary, we have reported the first example of transition-metal-catalyzed bond formation selectively at targeted organs within a live animal. The success of this transformation was dependent on both the usage of albumin as a metal complex carrier (owing to the strong affinity of coumarin derivatives to the hydrophobic binding pocket) and as a targeting vessel (as in our previous strategy with N-glycocluster linkages). The Au<sup>III</sup> complexes were rapidly immobilized at glycan-targeted organs (within 30 min to the liver and intestine) without leaching or deactivation of the metal catalysts. Finally, target-selective labeling was shown by gold-catalyzed amide bond formation between fluorescent propargyl ester probes and amines on surface proteins of target organ tissues.

The significance of these results to the growing field of biologically active metal complex catalysts is that it presents a possible platform for metal complexes to be utilized in higher-level organisms. If successful, novel biomedical applications could be developed based upon transition-metal-catalyzed transformations. Exemplary therapies may include the uncaging of active, cancer therapeutic enzymes selectively at tumor sites or bioorthogonal cross-coupling reactions to produce active drug molecules at targeted organs. Currently, different N-glycan structures are being explored, with the hope that a larger selection of targeted organs, and possibly tumor tissues, can soon be fully encompassed with our method.

### Acknowledgements

This work was supported by JSPS KAKENHI Grants (JP16H03287, JP16K13104, and JP15H05843) in Middle Molecular Strategy and by a subsidy from the Russian Government "Program of Competitive Growth of Kazan Federal University among World's Leading Academic Centers". We thank Glytech, Inc. for supplying N-glycans.

### Conflict of interest

The authors declare no conflict of interest.

**Keywords:** amide bond formation · fluorescent labeling · glycoalbumin · gold catalysis

- [1] a) P. K. Sasmal, C. N. Streu, E. Meggers, *Chem. Commun.* **2013**, 49, 1581–1587; b) T. Völker, E. Meggers, *Curr. Opin. Chem. Biol.* **2015**, 25, 48–54; c) J. Li, P. R. Chen, *ChemBioChem* **2012**, 13, 1728–1731; d) M. Yang, J. Li, P. R. Chen, *Chem. Soc. Rev.* **2014**, 43, 6511–6526; e) S. V. Chankeshwara, E. Indrigo, M. Bradley, *Curr. Opin. Chem. Biol.* **2014**, 21, 128–135.
- [2] a) C. Streu, E. Meggers, *Angew. Chem. Int. Ed.* **2006**, 45, 5645–5648; *Angew. Chem.* **2006**, 118, 5773–5776; b) T. Völker, F. Dempwolff, P. L. Graumann, E. Meggers, *Angew. Chem. Int. Ed.* **2014**, 53, 10536–10540; *Angew. Chem.* **2014**, 126, 10705–10710; c) P. K. Sasmal, S. Carregal-Romero, W. J. Parak, E. Meggers, *Organometallics* **2012**, 31, 5968–5970; d) M. I. Sánchez, C. Penas, M. E. Vázquez, J. L. Mascareñas, *Chem. Sci.* **2014**, 5, 1901–1907.
- [3] K. K. Sadhu, E. Lindberg, N. Winssinger, *Chem. Commun.* **2015**, 51, 16664–16666.
- [4] P. K. Sasmal, S. Carregal-Romero, A. A. Han, C. N. Streu, Z. Lin, K. Namikawa, S. L. Elliott, R. W. Köster, W. J. Parak, E. Meggers, *ChemBioChem* **2012**, 13, 1116–1120.
- [5] J. Wang, S. Zheng, Y. Liu, Z. Zhang, Z. Lin, J. Li, G. Zhang, X. Wang, J. Li, P. R. Chen, *J. Am. Chem. Soc.* **2016**, 138, 15118–15121.
- [6] a) J. Li, J. Yu, J. Zhao, J. Wang, S. Zheng, S. Lin, L. Chen, M. Yang, S. Jia, X. Zhang, P. R. Chen, *Nat. Chem.* **2014**, 6, 352–361; b) J. Wang, B. Cheng, J. Li, Z. Zhang, W. Hong, X. Chen, P. R. Chen, *Angew. Chem. Int. Ed.* **2015**, 54, 5364–5368; *Angew. Chem.* **2015**, 127, 5454–5458; c) E. Indrigo, J. Clavadetscher, S. V. Chankeshwara, A. Lilienkamp, M. Bradley, *Chem. Commun.* **2016**, 52, 14212–14214; d) J. T. Weiss, J. C. Dawson, C. Fraser, W. Rybski, C. Torres-Sánchez, M. Bradley, E. E. Patton, N. O. Carragher, A. Unciti-Broceta, *J. Med. Chem.* **2014**, 57, 5395–5404; e) J. T. Weiss, J. C. Dawson, K. G. Macleod, W. Rybski, C. Fraser, C. Torres-Sánchez, E. E. Patton, M. Bradley, N. O. Carragher, A. Unciti-Broceta, *Nat. Commun.* **2014**, 5, 3277.
- [7] a) A. Unciti-Broceta, E. M. V. Johansson, R. M. Yusop, R. M. Sanchez-Martin, M. Bradley, *Nat. Protoc.* **2012**, 7, 1207–1218; b) R. M. Yusop, A. Unciti-Broceta, E. M. V. Johansson, R. M. Sánchez-Martín, M. Bradley, *Nat. Chem.* **2011**, 3, 239–243.
- [8] C. D. Spicer, T. Triemer, B. G. Davis, *J. Am. Chem. Soc.* **2012**, 134, 800–803.
- [9] a) N. Li, R. K. V. Lim, S. Edwardraja, Q. Lin, *J. Am. Chem. Soc.* **2011**, 133, 15316–15319; b) J. Li, S. Lin, J. Wang, S. Jia, M. Yang, Z. Hao, X. Zhang, P. R. Chen, *J. Am. Chem. Soc.* **2013**, 135, 7330–7338.
- [10] a) M. Jung Jou, X. Chen, K. M. K. Swamy, H. Na Kim, H.-J. Kim, S.-g. Lee, J. Yoon, *Chem. Commun.* **2009**, 7218–7220; b) J.-B. Wang, Q.-Q. Wu, Y.-Z. Min, Y.-Z. Liu, Q.-H. Song, *Chem. Commun.* **2012**, 48, 744–746; c) Y.-K. Yang, S. Lee, J. Tae, *Org. Lett.* **2009**, 11, 5610–5613; d) J. H. Do, H. N. Kim, J. Yoon, J. S. Kim, H.-J. Kim, *Org. Lett.* **2010**, 12, 932–934.
- [11] J. Clavadetscher, S. Hoffmann, A. Lilienkamp, L. Mackay, R. M. Yusop, S. A. Rider, J. J. Mullins, M. Bradley, *Angew. Chem. Int. Ed.* **2016**, 55, 15662–15666; *Angew. Chem.* **2016**, 128, 15891–15895.
- [12] B. W. Michel, A. R. Lippert, C. J. Chang, *J. Am. Chem. Soc.* **2012**, 134, 15668–15671.
- [13] a) A. Ogura, T. Tahara, S. Nozaki, K. Morimoto, Y. Kizuka, S. Kitazume, M. Hara, S. Kojima, H. Onoe, A. Kurbangalieva, N. Taniguchi, Y. Watanabe, K. Tanaka, *Sci. Rep.* **2016**, 6, 21797; b) A. Ogura, T. Tahara, S. Nozaki, H. Onoe, A. Kurbangalieva, Y. Watanabe, K. Tanaka, *Bioorg. Med. Chem. Lett.* **2016**, 26, 2251–2254; c) K. Tanaka, *Org. Biomol. Chem.* **2016**, 14, 7610–7621; d) L. Latypova, R. Sibgatullina, A. Ogura, K. Fujiki, A. Khabibrakhmanova, T. Tahara, S. Nozaki, S. Urano, K. Tsubokura, H. Onoe, Y. Watanabe, A. Kurbangalieva, K. Tanaka, *Adv. Sci.* **2016**, 1600394; e) K. Tanaka, K. Fukase, S. Katsumura, *Synlett* **2011**, 2115–2139; f) K. Tanaka, T. Masuyama, K. Hasegawa, T. Tahara, H. Mizuma, Y. Wada, Y. Watanabe, K. Fukase, *Angew. Chem. Int. Ed.* **2008**, 47, 102–105; *Angew. Chem.* **2008**, 120, 108–111; g) K. Tanaka, S. Katsumura, *J. Am. Chem. Soc.* **2002**, 124, 9660–9661.
- [14] K. Tanaka, K. Fukase, *Org. Biomol. Chem.* **2008**, 6, 815–828.
- [15] a) K. J. Fehske, U. Schläfer, U. Wollert, W. E. Müller, *Mol. Pharmacol.* **1982**, 21, 387–393; b) A. M. L. Zatón, J. M. Ferrer, J. C. R. de Gordo, M. A. Marquinez, *Chem.-Biol. Interact.* **1995**, 97, 169–174; c) A. Garg, D. Mark Manidhar, M. Gokara,

- C. Malleda, C. Suresh Reddy, R. Subramanyam, *PLOS ONE* **2013**, *8*, e63805.
- [16] a) Y. Fuchita, H. Ieda, Y. Tsunemune, J. Kinoshita-Nagaoka, H. Kawano, *J. Chem. Soc. Dalton Trans.* **1998**, 791–796; b) K. K.-Y. Kung, V. K.-Y. Lo, H.-M. Ko, G.-L. Li, P.-Y. Chan, K.-C. Leung, Z. Zhou, M.-Z. Wang, C.-M. Che, M.-K. Wong, *Adv. Synth. Catal.* **2013**, *355*, 2055–2070; c) K. K.-Y. Kung, H.-M. Ko, J.-F. Cui, H.-C. Chong, Y.-C. Leung, M.-K. Wong, *Chem. Commun.* **2014**, *50*, 11899–11902.
- [17] a) C. Bruneau, Z. Kabouche, M. Neveux, B. Seiller, P. H. Dixneuf, *Inorg. Chim. Acta* **1994**, *222*, 155–163; b) N. Ghosh, S. Nayak, A. K. Sahoo, *J. Org. Chem.* **2011**, *76*, 500–511.
- [18] E. I. Park, Y. Mi, C. Unverzagt, H.-J. Gabius, J. U. Baenziger, *Proc. Natl. Acad. Sci. USA* **2005**, *102*, 17125–17129.

Manuscript received: October 20, 2016

Revised: December 14, 2016

Final Article published: ■ ■ ■ ■, ■ ■ ■ ■

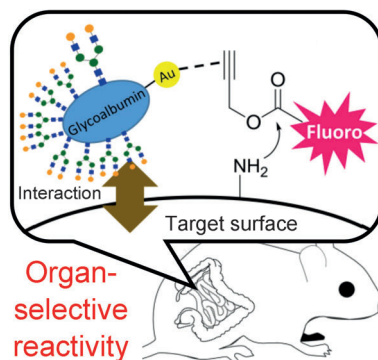
## Communications



## Fluorescent Labeling

K. Tsubokura, K. K. H. Vong,  
A. R. Pradipta, A. Ogura, S. Urano,  
T. Tahara, S. Nozaki, H. Onoe, Y. Nakao,  
R. Sibgatullina, A. Kurbangalieva,  
Y. Watanabe, K. Tanaka\* — ■■■■—■■■■

In Vivo Gold Complex Catalysis within  
Live Mice



The first metal-catalyzed reaction that proceeds within live mice is based on a targeting approach with glycans. Glycoalbumin–Au<sup>III</sup> complexes can be accumulated in specific organs where they catalyze amide bond formation between a propargyl ester probe and amine groups on nearby proteins. The selective targeting was confirmed by whole body fluorescence imaging and analysis of dissected tissues.